

High-pressure sensor using piezoelectric bending resonators

Xiaoqi Bao¹, Stewart Sherrit and Nobuyuki Takano

Jet Propulsion Laboratory, California Institute of Technology, Pasadena, CA 91109, USA

ABSTRACT

A novel design of pressure sensor based on piezoelectric bending resonator is described in this paper. The resonator is isolated from and mechanically coupled to the surrounding fluid using a sealed enclosure. The pressure applied to the enclosure induces a compressive stress to the resonator and reduces its resonance frequency. In principle the mechanism allows for achieving large resonance frequency shifts close to 100% of the resonance frequency. A high-pressure sensor based on the mechanism was designed for down-hole pressure monitoring in oil wells. The sensor is potentially remotely-readable via the transmission of an electromagnetic signal down a waveguide formed by the pipes in the oil well. The details of the pressure sensor design and verification by FE analysis and initial test results of a preliminary prototype are presented in this paper.

KEYWORD: piezoelectric, pressure sensor, down-hole oil wells, passive, remotely readable.

1. INTRODUCTION

Oil industries need a passive (no local power supply) downhole high-pressure sensors that are readable remotely from surface using downhole communication technology e.g. INFICOMM™ [Los Alamos National Laboratory, 2012]. The INFICOMM™ system uses concentric pipes downhole as an electromagnetic waveguide. The system requires the resonator pressure sensors have pressure measurement range up to 20-200MPa, minimum electric impedance at resonance frequency <50 Ohm and operate in low RF range of 5 – 200 kHz.

The novel bending-resonator pressure sensor described in this paper consists of a piezoelectric bending resonator which has a resonance in low RF frequency range and a high-pressure enclosure which contains, seals and is mechanically coupled to the resonator. The mechanical coupling enables the resonance frequency of the resonator to sense the pressure outside the enclosure. Using high performance piezoelectric ceramic material and an enclosure to keep the resonator surrounded by low pressure air the resonator maintains high mechanical Q and low electric impedance at resonance.

A schematic of a piezoelectric bending-resonator sensor is presented in **Figure 1**. It has a cylindrical enclosure consisting of a tube and two caps made of high strength alloy. Two piezoelectric ceramic disks are fixed on a circular metal plate to form a bending resonator. The disks could be fixed on the surfaces of the plate or embedded in the plate as shown in the figure to reduce the shear stress in the joint interfaces when pressure is applied at the outer edge of the plate. The disks were poled in the same direction (nominally both up). Each piezoelectric disk has one electrode electrically contacted to the plate which is connected to ground. The other electrodes are

¹ Correspondence: xbao@jpl.nasa.gov

connected together to the terminal of the sensor. These electrical connections allow an efficient coupling between the electric signals at the terminal to the bending vibration of the resonator. When the thickness of the resonator is relatively thin the boundary condition of the bending vibration is close to clamped and the resonance frequencies are determined by the mass and bending stiffness of the plate resonator if no pre-stress applied. Similar to the wires in piano, a tensional pre-stress will increase the resonance frequency. Inversely a compressional in-plane stress decreases the frequency of the resonator. Since the wall of the enclosure is elastic a compressional in-plane stress will be induced in the resonator in a high-pressure environment. It is expected the resonance frequency of the resonator will decrease with the increase in external pressure. Theoretically the low limit of the frequency of the first mode is zero corresponding to the buckling point of the plate [Wah, 1962].

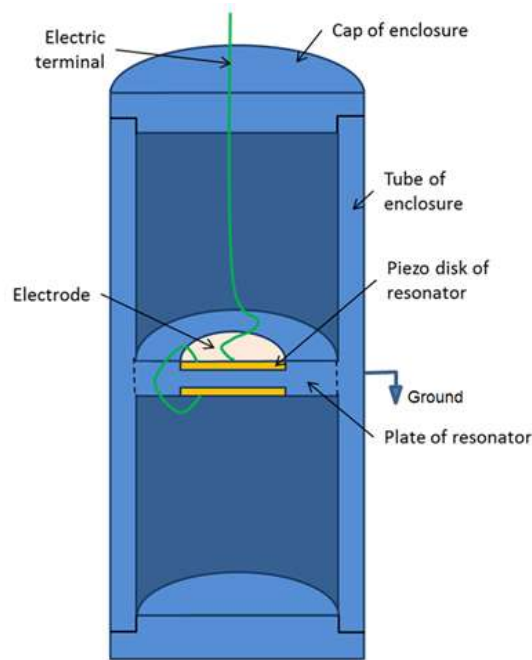


Figure 1: Schematic of a high-pressure sensor using piezoelectric bending resonator (not scaled)

2. FEASIBILITY AND DESIGN PARAMETER STUDY

The feasibility of the high-pressure sensors based on the mechanism described above was investigated by finite element (FE) modeling. Design parameter study was performed for the sensor with cylindrical enclosures. Model simulations were conducted for the configuration that is shown in **Figure 1** with various bending resonator thicknesses. The material of the enclosure and the plate in the simulated model is Titanium alloy Ti-6Al-4V and the piezoelectric disk material is PZT-8. The sensor enclosure is 25 mm in diameter and 60 mm in length. The detailed dimensions are presented in **Figure 2**. The total thickness of the resonator was investigated from 2 mm to 0.58 mm while the thickness of the piezoelectric disks is $\frac{1}{4}$ of the total thickness. The diameters of the PZT disks are 0.7 of the diameter of the resonator. All the joints are assumed to be zero bond thickness. The first bending mode shape for the case of 1-mm thick resonator and zero external pressure is illustrated in **Figure 3**. The resonance frequency is 18.586 kHz and, as expected, the displacement of the enclosure is small and most vibration energy is in the resonator. By assuming a reasonable

overall mechanical Q of 500 the electric impedance is calculated and presented in **Figure 4**. The predicted minimum impedance at resonance frequency is 30 Ohm that is within desired range for nominal transmission lines.

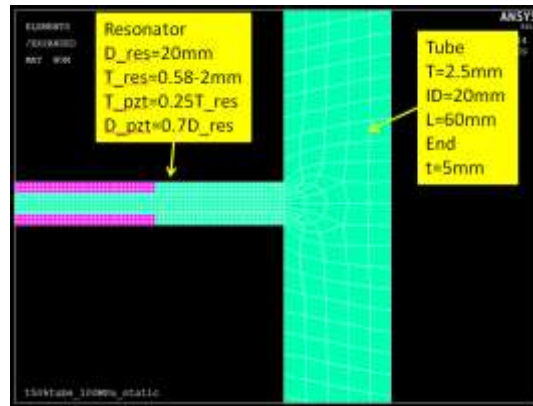


Figure 2: Dimensions of the simulated sensor with various resonator thickness and partial mesh of the FE model.

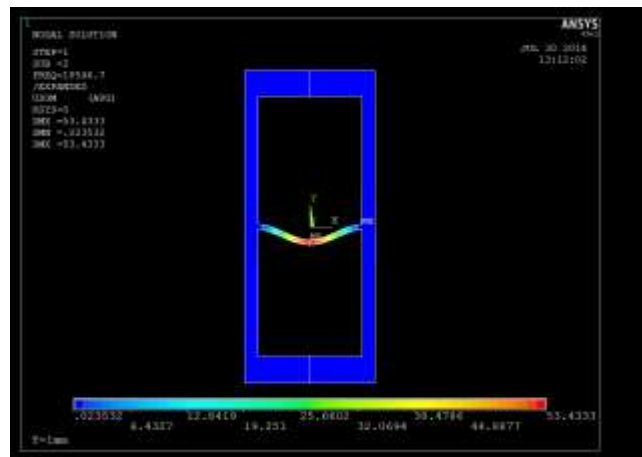


Figure 3: FE result of the first bending vibration mode (18.5 kHz) of the resonator with thickness of 1-mm at 0 MPa pressure.

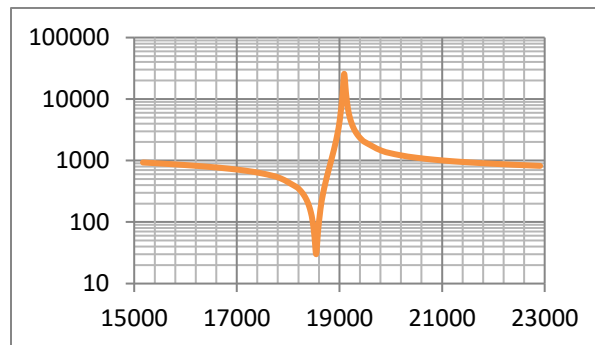


Figure 4: Impedance of the resonator with thickness of 1-mm assuming $Q_m = 500$.

The deformation, induced stress and resonance frequency shift were computed with external pressure up to 100 MPa. The deformation and stress in the sensor with 1-mm thick resonator under external pressure of 100 MPa are presented in **Figure 5**. A compressional stress is induced to the resonator. **Figure 6** shows the resonance frequencies and frequency shifts by external pressure of 100 MPa as functions of thicknesses of the resonator while keeping the thickness of PZT disks at a constant ratio of 0.25 to the total thickness. The data are also listed in **Table 1**. The results show the resonance frequencies drop gradually with the decrease of the thickness at zero pressure. For all calculated resonator thicknesses the resonance frequencies shift to lower values under pressure. And, the less the thickness is, the larger the frequency shift will be. For the thickness of 0.58 mm the resonance frequency drops more than 90% at the pressure of 100 MPa. The compressional stress in the resonator is close to the buckling point in this case. The modeling results confirmed that a large frequency shift is possible for this bending-resonator pressure sensor.

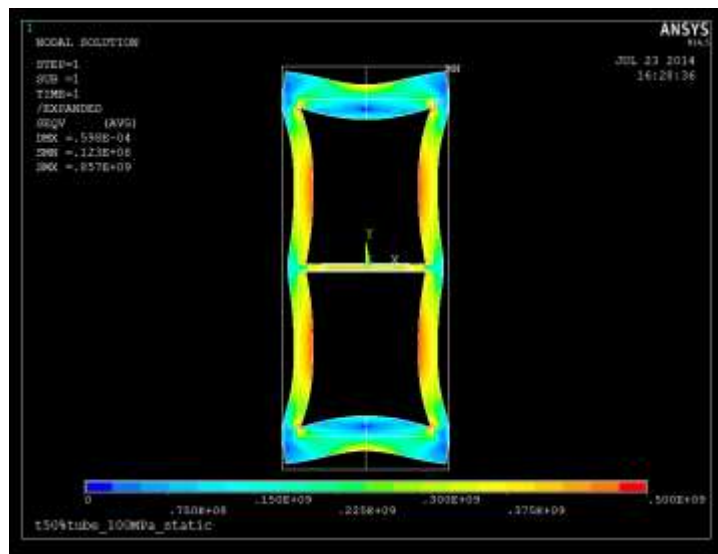


Figure 5: Deformation and von Mises stress in the sensor with 1-mm thick resonator under 100 MPa external pressure.

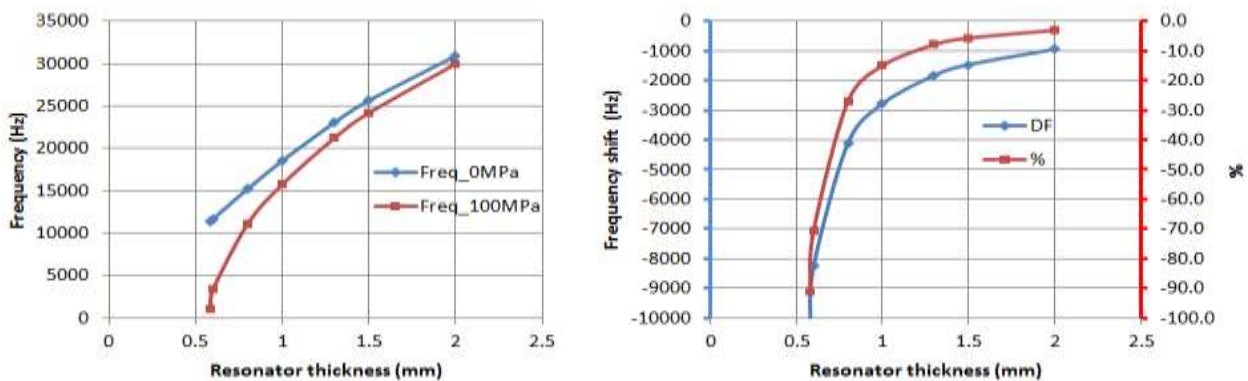


Figure 6: Resonance frequencies and frequency shifts under pressure as functions of resonator thicknesses

Table 1: Resonance frequencies and minimum impedances for various resonator thicknesses

Thickness (mm)	Freq_0MPa	Freq_100MPa	ΔF (Hz)	%	Z_{min} (Ω)
2	30919	29973	-946	-3.1	38
1.5	25644	24178	-1466	-5.7	33
1.3	23042	21212	-1830	-7.9	32
1	18547	15763	-2784	-15.0	30
0.8	15231	11131	-4100	-26.9	30
0.6	11697	3435	-8262	-70.6	29
0.58	11317	1021	-10296	-91.0	29

Another set of simulations were conducted for various thickness of piezoelectric disks while keeping the total thickness of the resonator constant (1 mm). The FE model also includes epoxy bonding interfaces between the piezoelectric disks and the Ti plate. The thickness of the bonding interfaces is set as 10 μm . The losses of materials are also included in the model. Instead of assuming an overall mechanical Q of 500 for the bending mode in the previous simulations the mechanical Q of the resonance mode is calculated by the FE model. The corresponding mechanical Q of titanium alloy, PZT and epoxy are set as 1000, 500 and 10, respectively.

The frequency shift for a 100 MPa change in pressure and the calculated impedance at resonance are shown in **Figure 7** as functions of the thickness of the PZT disks. More detailed data are listed in **Table 2**. The results show the benefits of use thin PZT disks in the evaluated range. Although the percentage of frequency shift reaches maximum at PZT thickness of 0.25 mm the variation is not significant (14.6% to 15.3%) for the studied thickness range from 0.1 mm to 0.35 mm. The resonance frequency shift is seen to increase with the decrease of the PZT thickness and the minimum impedance is also lower with thinner PZT disks.

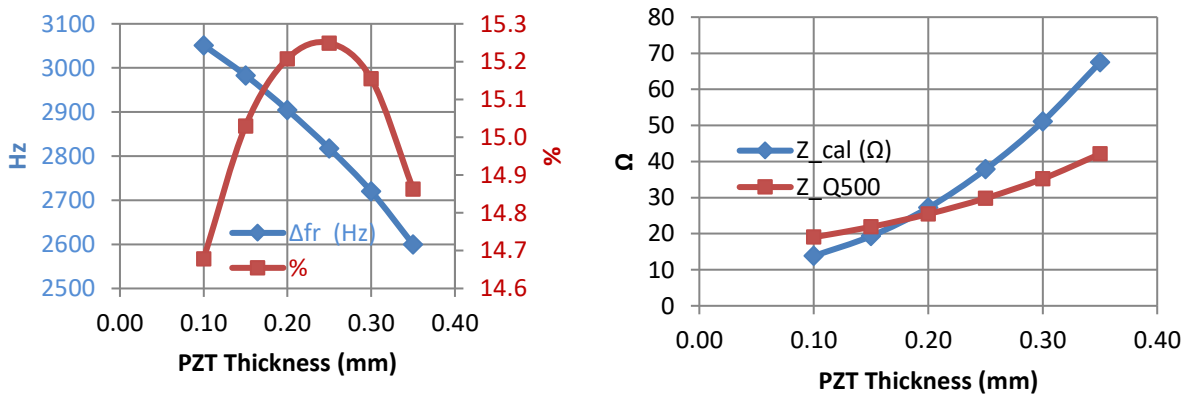


Figure 7: The frequency shift and the percent frequency shift for a 100 MPa change in pressure (left) and the impedance at resonance calculated from the material Qs (right) as functions of the PZT disc thickness. The impedances calculated based on overall Q of 500 are also presented for comparison.

Table 2: Resonance frequencies and minimum impedances for various PZT thicknesses while total resonator thickness is 1 mm.

T_pzt (mm)	C0 (F)	fr (Hz)	fa (Hz)	Z_cal (Ω)	Q_cal	Z_Q500	fr_100MPa (Hz)	fa_100MPa (Hz)	Δ fr (Hz)	%
0.10	2.46E-08	20787	21137	13.8	688	19.0	17736	18144	3051	14.7
0.15	1.66E-08	19848	20300	19.3	566	21.9	16865	17393	2983	15.0
0.20	1.26E-08	19100	19615	27.2	468	25.4	16195	16796	2905	15.2
0.25	1.02E-08	18476	19024	37.8	394	29.8	15659	16296	2817	15.2
0.30	8.52E-09	17948	18504	51.1	345	35.2	15228	15872	2720	15.2
0.35	7.31E-09	17493	18035	67.4	312	42.1	14893	15519	2600	14.9

3. SENSOR PROTOTYPE FOR TEST

A test prototype sensor was fabricated to verify the results of the FE model. Commercial-off-shelf PZT disks were used. The disks are APC841 piezoceramic [APC, 2016] with 10 mm diameter and 0.2 mm in thickness. The FE model was used to help the prototype design. The design was iterated to reduce critical stresses in the various components especially in the epoxy join layer. The dimensions of the iterated design are presented in **Figure 8** which shows the mesh of the FE model for the prototype. The FE predicted performances are listed in **Table 3**.

The Ti plate of the resonator and the tube of enclosure are manufactured as one piece for a good connection between the resonator and the enclosure. A high temperature epoxy is used to assemble the PZT disks and the end caps. High-pressure wire feedthroughs are mounted on both end caps with thread and O-ring seal. The outside electrodes of the two PZT disks are connected to the two feedthroughs respectively and connected together outside the enclosure for the test. The assembled prototype sensor is shown in **Figure 9**.

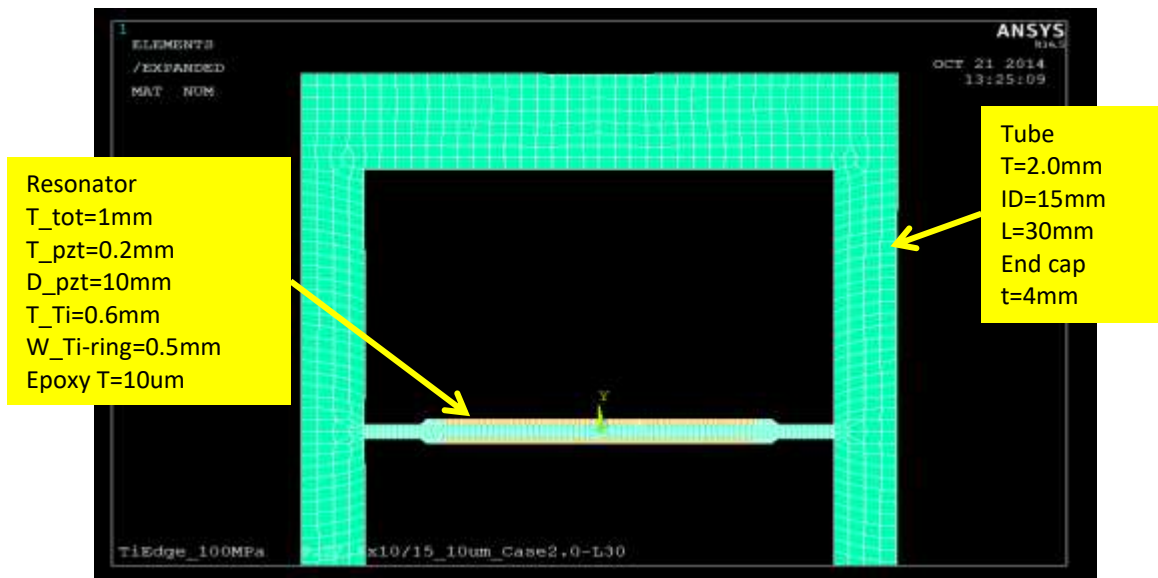


Figure 8: Dimensions of the prototype sensor design

Table 3: FE prediction and the measured data of the test sensor with no end caps

	C ₀ (F)	f _r (Hz)	f _a (Hz)	k	Z (Ω)	Q _m	f _{r_100MPa} (Hz)	Δf _r (Hz)	%
FE	6.97E-09	23826	25226	0.329	17.4	510	20567	3259	13.7
Measured	5.39E-09	26241	27529	0.302	32.8	376			



Figure 9: The prototype sensor

The impedance spectrum for the device without endcaps is shown in **Figure 10**. A resistance at resonance frequency of 26.25 kHz is about 33 Ohms which meets the requirement (≤ 50 Ohms). The corresponding mechanical Q is around 337. The data from the impedance spectrum measurement are listed in **Table 3** and compared with the FE model prediction. The experimental data are in general agreement with the results of the FE model. The fillet at the corner of the resonator and tube may result in the 10% higher resonance frequency found in the prototype over the model prediction. The lower Q and higher impedance of the prototype may be caused by a thicker bonding layer in assembly. **Figure 11** shows the impedance spectra with endcaps glued to the cylinder and the electric feedthroughs mounted with an O-ring. The minimum impedance rose to 120 Ohms and the mechanic Q dropped to 105 correspondingly. It is believed that the losses of the glue at the endcaps and the O-ring, which have not been accounted for in the FE model, are responsible for the drop in Q. This suggests that the method to secure and seal the endcaps and feedthroughs need to be improved to reduce these interface losses.

With the whole device immersed in Shell Tellus oil we found the impedance at resonance was increased about 7 percent which suggests that the sensor structure is not completely decoupled from the outer housing and results in additional loss in viscous oil. Design parameter and structure changes may reduce the loss. The pressure sensitivity will be measured when suitable high-pressure test setup is ready for testing. In addition, more tests are needed to evaluate the full performances of the sensor such as stability, temperature effects, durability, etc.

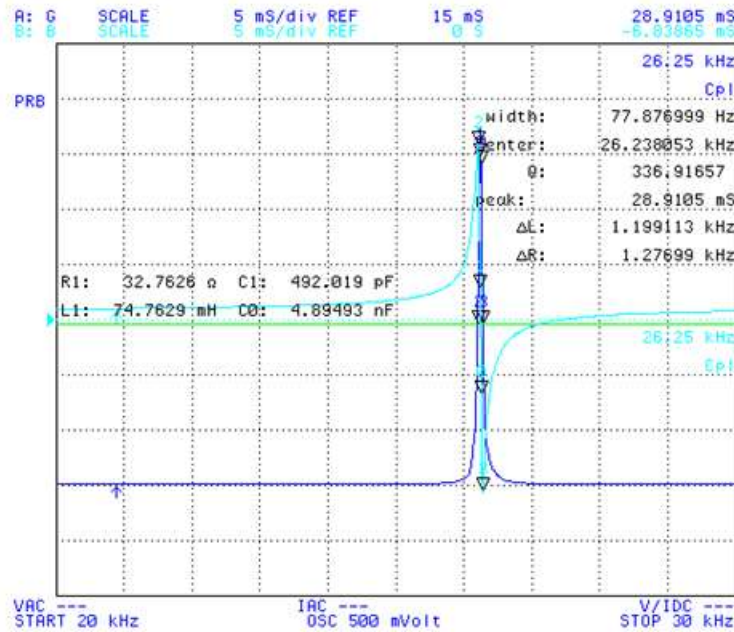


Figure 10: The impedance spectra of the assembled resonator without endcaps

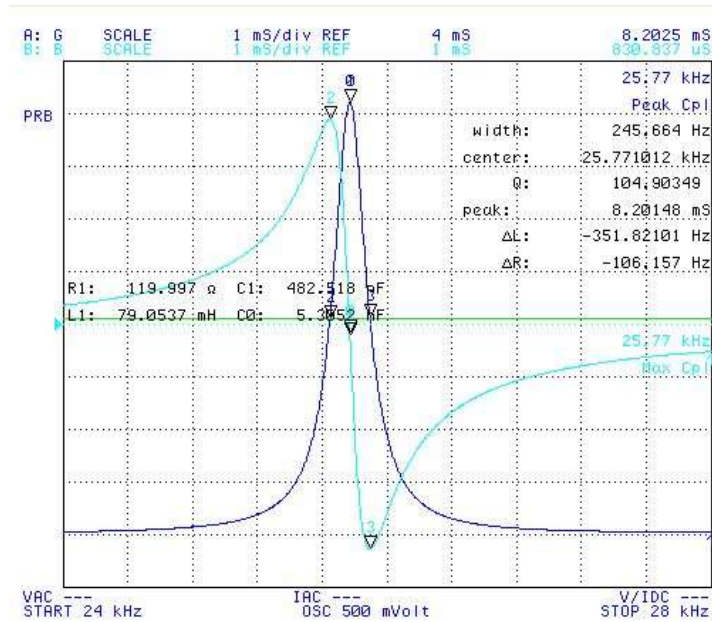


Figure 11: The impedance spectra of the assembled resonator with endcaps

4. SUMMARY

This paper reports a novel high-pressure sensor design using a piezoelectric bending resonator. The resonator is mounted inside of a sealed high-pressure enclosure and senses the outside pressure changes by resonance frequency shifts caused by the in-plane stress change induced by the pressure through the wall of the enclosure. Large frequency shifts are achievable for the sensors designed based on this mechanism. The sensors can be operated at low RF range and have impedances that

are below that of the transmission line formed by pipelines in oil wells and, therefore, potentially allow remote reading through long distance.

The performances of the sensor designs were evaluated by FE modeling. A test device was fabricated and preliminary tests confirmed the general predictions of the FE model. More tests are needed to evaluate the test sensor and further developments are required to improve the sensor designs and fabrication procedures.

ACKNOWLEDGMENT

Research reported in this manuscript was conducted at the Jet Propulsion Laboratory (JPL), California Institute of Technology, under a contract with National Aeronautics Space Administration (NASA).

REFERENCES

- APC International, Ltd, "Physical and piezoelectric properties of APC materials", <https://www.americanpiezo.com/apc-materials/physical-piezoelectric-properties.html>, last visit Feb. 2016
- Los Alamos Laboratory, "Wireless technology collects real-time information from oil and gas wells," <http://www.lanl.gov/about/stories/wireless-technology-collects-real-time-information-from-oil-and-gas-wells.php>, last visit Feb. 2016, (2012)
- Wah, Thein, "Vibration of Circular Plates," J. ASA, vol. 34, no. 3, Mar., pp. 275-281 (1962).